ACCSCIENCE PUBLISHING

Journal of Chinese Architecture and Urbanism

ORIGINAL ARTICLE

Zonal variation in commercial function–human activity relationships around North Ring Road Station, Changchun: Evidence from sampled weekday and weekend conditions

Danwei Zhao[1,2], Ahmad Nurfaidhi Rizalman[3]*, Linxi Zeng[2], Qiuyu Zhao[2], and Pengbo Li[2]

[1]Faculty of Engineering, Universiti Malaysia Sabah, Sabah, Kota Kinabalu, Malaysia

[2]College of Forestry, Beihua University, Jilin City, China

[3]Nanomaterials Research Centre, Faculty of Engineering, Universiti Malaysia Sabah, Kota Kinabalu, Malaysia

***Corresponding author:**
Ahmad Nurfaidhi Rizalman
(ahmadnurfaidhi@ums.edu.my)

Citation: Zhao, D., Rizalman, A. N., Zeng, L., Zhao, Q., & Li, P. (2026). Zonal variation in commercial function–human activity relationships around North Ring Road Station, Changchun: Evidence from sampled weekday and weekend conditions. *Journal of Chinese Architecture and Urbanism*. 8(4):026340053. doi: 10.36922/JCAU026340053

Received: August 19, 2026

Revised: October 3, 2026

Accepted: October 15, 2026

Published online: November 2, 2026

Copyright: © 2026 Author(s). This is an Open-Access article distributed under the terms of the Creative Commons AttributionNon-Commercial 4.0 International (CC BY-NC 4.0), which permits all non-commercial use, distribution, and reproduction in any medium, provided the original work is properly cited.

Publisher's Note: AccScience Publishing remains neutral with regard to jurisdictional claims in published maps and institutional affiliations.

Abstract

Commercial concentration does not necessarily correspond to observed human activity in metro station areas, and temporal differences may occur through localized changes even when the overall activity structure remains stable. Identifying such internal restructuring is important because aggregate station-wide measures may overlook how specific commercial functions relate differently to human activity across spatial zones. North Ring Road Station in Changchun is examined within 800 m of its two operational entrances. A total of 951 commercial and service points of interest in seven categories are combined with Baidu-derived human activity intensity from one sampled weekday and one sampled weekend day. Data are integrated into 30 m analytical grids and divided into Core (0–300 m), Transitional (300–500 m), and Peripheral (500–800 m) zones. A standardized relative positional change indicator (ΔZ) tracks changes in each grid's relative position, and functional associations are assessed using Spearman correlations and spatial block bootstrap. The overall commercial function–activity relationship remains broadly similar across the two sampled days, whereas clearer internal differences emerge. Mean ΔZ is −0.085 in the Core Zone and +0.048 in the Peripheral Zone, with a small overall zonal effect ($\varepsilon^2 = 0.015$). Shopping, food and beverage, daily life services, sports and recreation, and healthcare show clearer core-to-peripheral shifts in their associations with ΔZ. Because the observations are limited to one sampled weekday and one sampled weekend day, the identified differences reflect the two sampled conditions and should not be generalized to broader weekday–weekend patterns. These findings provide sampled-day evidence of localized functional restructuring within a broadly stable activity pattern and demonstrate the value of zonal and function-specific analysis beyond aggregate station-wide measures.

Keywords: Human activity intensity; Commercial functions; Metro station area; Zonal heterogeneity; Relative spatial change; Point of interest

1. Introduction

Rail transit station areas serve not only as transport hubs, but also as important urban spaces where commercial services and routine activities tend to cluster. As rail transit becomes more closely integrated with surrounding urban functions, accessibility and commercial provision are often improved at the same time. However, this does not always lead to a comparable increase in human activity or space use. Transit-oriented development and node–place theory both emphasize the coordination of transport conditions, functional configuration, and place value (Bertolini, 1999; Calthorpe, 1993; Cervero & Kockelman, 1997). In practice, these elements may not develop at the same pace. Commercial concentration does not always correspond to higher observed human activity, although human activity is an important observable dimension of station-area vitality. In station areas, facility density or development intensity may therefore capture only part of actual space use.

Functional provision and actual use also vary over time. Weekday activity is often associated with commuting and routine needs, whereas consumption and leisure become more prominent on weekends and may alter the spatial relationship between commercial functions and observed activity (Tang & Ta, 2022; B. Wang *et al.*, 2022; Wu *et al.*, 2018). These changes need not involve a major shift in the overall activity pattern. A station-area center may remain stable while individual locations change in relative prominence, or while the association between a particular commercial function and human activity varies across space. Such local changes can be difficult to detect from station-wide averages alone. Distance is only part of this process. Spatial connections within the station area also depend on metro entrance locations, street layout, road barriers, and surrounding land use (Lahoorpoor & Levinson, 2020; Yan *et al.*, 2024). Commercial functions themselves differ in use patterns. Shopping, food and beverage, daily life services, sports and recreation, and healthcare serve different needs, attract different users, and operate at different times. Their relationships with observed human activity may therefore vary by location, while total commercial density or overall functional diversity can obscure some of these differences (Yue *et al.*, 2017).

For this reason, the two sampled days are treated as contrasting observational conditions rather than as statistically representative weekday and weekend populations. The purpose of the comparison is not to establish a general weekday–weekend temporal pattern, but to examine whether a broadly similar station-area activity structure can contain localized differences in relative spatial position and function-specific associations. Individual locations may gain or lose relative prominence between the two observations even when the main activity center remains unchanged. At the intra-station scale, these differences may also vary between areas close to station entrances and those farther away. Accordingly, the analysis examines whether the overall relationship between commercial functions and human activity remains similar across the two sampled days, whether localized differences become more evident when spatial zones and commercial functions are considered separately, and whether the observed differences follow a simple distance-based pattern or are more closely associated with local spatial context.

North Ring Road Station in Changchun is used as the case study. Data on commercial and service points of interest (POIs) represent functional concentration, while Baidu-derived human activity intensity is used to describe observed activity and is treated as an empirical indicator related to station-area vitality, rather than as a direct measure of commercial vitality. Spatial zones are defined according to the station's operational entrances. Using observations from one sampled weekday and one sampled weekend day, the analysis first compares the overall relationship between commercial functions and human activity intensity. This comparison is exploratory and is limited to the two sampled conditions. It then examines changes in the relative position of spatial units across different functions and zones. This combination of station-wide and zonal analysis makes it possible to identify local functional differences that may remain less visible in aggregate comparisons and provides a finer-grained view of commercial function–activity relationships around a metro station.

2. Literature review and theoretical framework

2.1. Relationship between commercial function provision and spatial vitality

Urban vitality does not necessarily increase in line with commercial facility density or development intensity. Jacobs (1961), Hillier *et al.* (1993), and Montgomery (1998) showed from the perspectives of functional diversity, street networks, and place quality that human activity is jointly shaped by functional provision, spatial organization, accessibility, and public space conditions. Later empirical studies further found that commercial distribution is closely related to network position, agglomeration, and built-environment scale, while its relationship with urban vitality may also be nonlinear (Yinghong Jiang *et al.*, 2022; Peng *et al.*, 2023; Sevtsuk, 2014). Commercial concentration therefore indicates the spatial provision of activity opportunities, while observed human activity reflects actual space use. The relationship between the two

may also vary with spatial scale and local context (J. Duan *et al.*, 2025). The "high development with low vitality" and "low development with high vitality" patterns identified by Xia *et al.* (2020) further indicate potential mismatches between spatial provision and behavioral activity. In rail transit station areas, large blocks, road barriers, commercial frontages, and pedestrian connections may further reshape this relationship. Accordingly, analyses of station-area commercial space should consider not only where commercial functions are concentrated, but also how functional provision corresponds to observed human activity under different spatial contexts (Abudurexiti *et al.*, 2025).

2.2. Temporal rhythms and the dynamics of commercial space

Human activity in commercial and transit spaces varies across temporal conditions. Commuting, employment, and routine needs tend to dominate weekday activity, while weekends often involve a greater share of consumption, leisure, and social use. Studies based on check-in records, Baidu heat maps, and other urban datasets have shown that temporal differences may appear both in activity concentration and in its relationship with POIs and built-environment conditions (Tang & Ta, 2022; B. Wang *et al.*, 2022; Wu *et al.*, 2018). At the station-area scale, Peng *et al.* (2023) and Guo *et al.* (2024) also reported temporal variation in the relationships among urban functions, spatial conditions, and human activity. Existing studies mainly compare differences in activity levels and their determinants. Less attention has been given to changes within an otherwise stable spatial structure. Individual locations may change their relative prominence even when the main activity center remains largely unchanged. Distinguishing these local changes from changes in the overall structure can therefore reveal temporal variation that is less visible in aggregate comparisons.

2.3. Station entrances, spatial zones, and internal heterogeneity

Rail transit station areas are commonly examined within 400–800 m of stations, but a uniform boundary does not imply homogeneous spatial relationships within that area. Street networks, land use, road barriers, and entrance locations all influence accessibility and activity connectivity (Bivina *et al.*, 2020; Moyano *et al.*, 2023). Lahoorpoor and Levinson (2020) and Yan *et al.* (2024) further pointed out that metro entrances reshape the effective service area, meaning that measurements based on the station's geometric center may obscure local differences. The relationship between urban functions and human activity is also scale-dependent, and the same function may show different associations across spatial extents and contexts (J. Duan *et al.*, 2025). Guo *et al.* (2024) found differences in street function and convenience at different distances, while Miao and Zhou (2025) showed that some transit-related activities extend beyond conventional station-area boundaries. C. Duan and Chen (2026) further identified a hierarchical radius structure for public life activities. These findings suggest that distance should not be treated as a simple linear attenuation factor. Entrance-based zones can instead provide a consistent analytical framework for examining internal variation, while their boundaries should be understood as analytical distance bands rather than direct representations of pedestrian catchments.

2.4. Literature synthesis and theoretical framework

Existing research has established that urban vitality and human activity vary across both time and space. Recent studies have also moved toward finer-grained, human-centered, and scale-sensitive approaches to urban spatial dynamics (Cai *et al.*, 2026; Cai, 2026; J. Duan *et al.*, 2025). For metro station areas, however, aggregate relationships can remain relatively stable while local spatial units change in relative position, and the same commercial function may relate differently to human activity across internal zones. These two forms of variation are difficult to capture through station-wide POI–vitality correlations alone. As shown in Figure 1, this study therefore examines the relationship between commercial functions and observed human activity at three connected levels. It first evaluates the overall correspondence under the two sampled conditions, then identifies changes in the relative position of spatial units using ΔZ, and finally compares function-specific associations across the core, transitional, and peripheral zones with spatial robustness tests. The framework is intended to distinguish overall stability from local positional and functional variation within the station area.

3. Study area, data, and methods

3.1. Study area

The North Ring Road Station, located in Kuancheng district, Changchun city, is an interchange station for Metro Lines 1 and 8. Two metro entrances are currently in operation, and an 800 m area around these entrances is used as the analytical station-area extent (Figure 2A). This boundary provides a consistent spatial basis for examining internal variation and is not intended to define the full catchment of major commercial destinations. Land use is mixed. Along with a large commercial complex and a specialty market in the north, the area contains residential neighborhoods, education and research facilities, administrative offices,

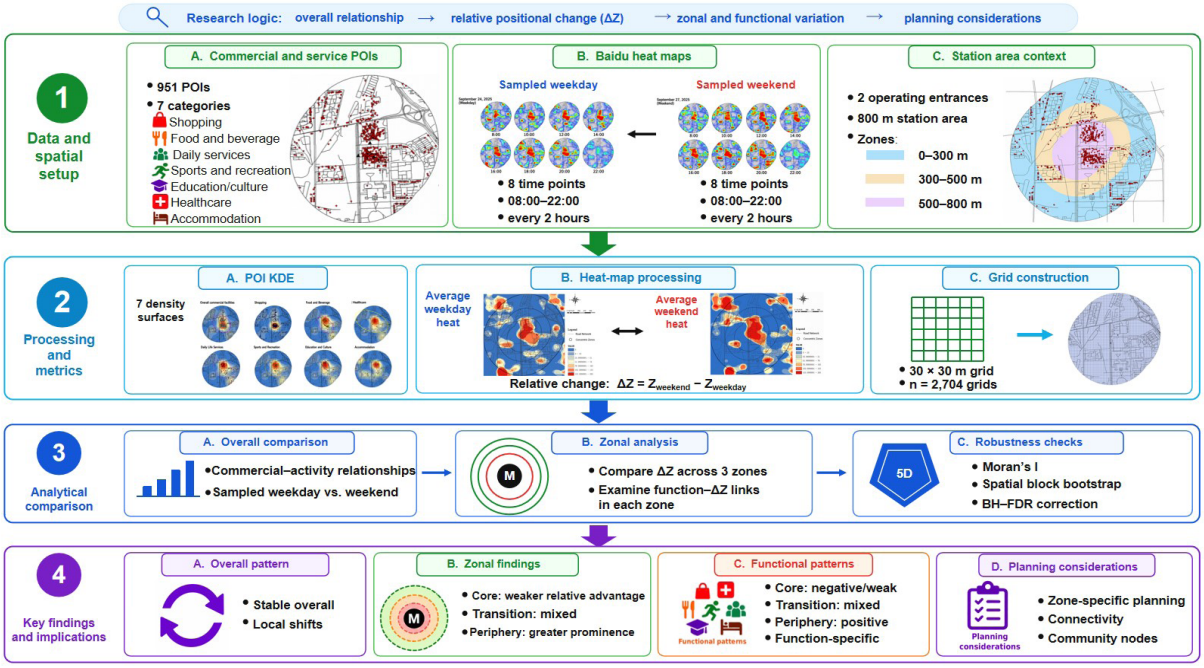


Figure 1. Research framework for zonal variation in commercial function–human activity relationships around North Ring Road Station, Changchun
Abbreviations: BH–FDR: Benjamini–Hochberg false discovery rate; KDE: Kernel density estimation; POI: Point of interest. Source: Diagram by the authors

public green space, and land reserved for or undergoing development.

As shown in Figure 2B, commercial and service land is concentrated around the station entrances and in the central area. Residential land is mainly distributed in the northwest, northeast, and southeast perimeters, while educational, research, and administrative land is concentrated in the central and southern areas. Overall, the station area forms a complex spatial structure consisting of a commercial core area, specialized market nodes, and surrounding residential areas. Major roads, large blocks, and relatively enclosed land use also limit the connectivity of local areas, resulting in significant functional differentiation and spatial heterogeneity. These characteristics make the area suitable for examining activity patterns under the two sampled conditions, changes in relative activity position, and differences in commercial functions across the core, transitional, and peripheral zones.

3.2. Data sources and processing

3.2.1. Commercial and service points of interest

Commercial and service POI data were obtained from the Amap Open Platform in June 2025. After spatial filtering, duplicate removal, category verification, and coordinate checking, 951 valid POIs were retained and classified into seven functional categories: shopping, food and beverage, daily life services, sports and recreation, education and culture, healthcare, and accommodation. All GCJ-02 coordinates were converted to WGS84 and projected to WGS 1984/UTM Zone 51N. Kernel density estimation (KDE) and standard deviational ellipse analyses were carried out in ArcGIS Desktop (10.8, Esri, USA) to examine spatial concentration, dominant orientation, and dispersion (Silverman, 2018). All POIs were given equal weight, and planar distance was used. For KDE, the cell size was 3 m, and the search radius was 300 m, which was used as a smoothing parameter to represent local commercial concentration. Density was measured in points/sqkm. The same projection, analysis extent, and raster alignment were used for all KDE surfaces. Density values were then extracted to 30 m × 30 m grids to represent the spatial concentration of the seven commercial functions.

3.2.2. Baidu heat maps and measurement of human activity intensity

Baidu heat maps indicate the spatial concentration and relative intensity of platform-detected human activity. In this study, the converted heat values characterize relative human activity intensity within the station area. Data were collected on September 24, 2025, a weekday, and September 27, 2025, a weekend day. Observations were taken every two hours from 08:00 to 22:00, producing eight observations

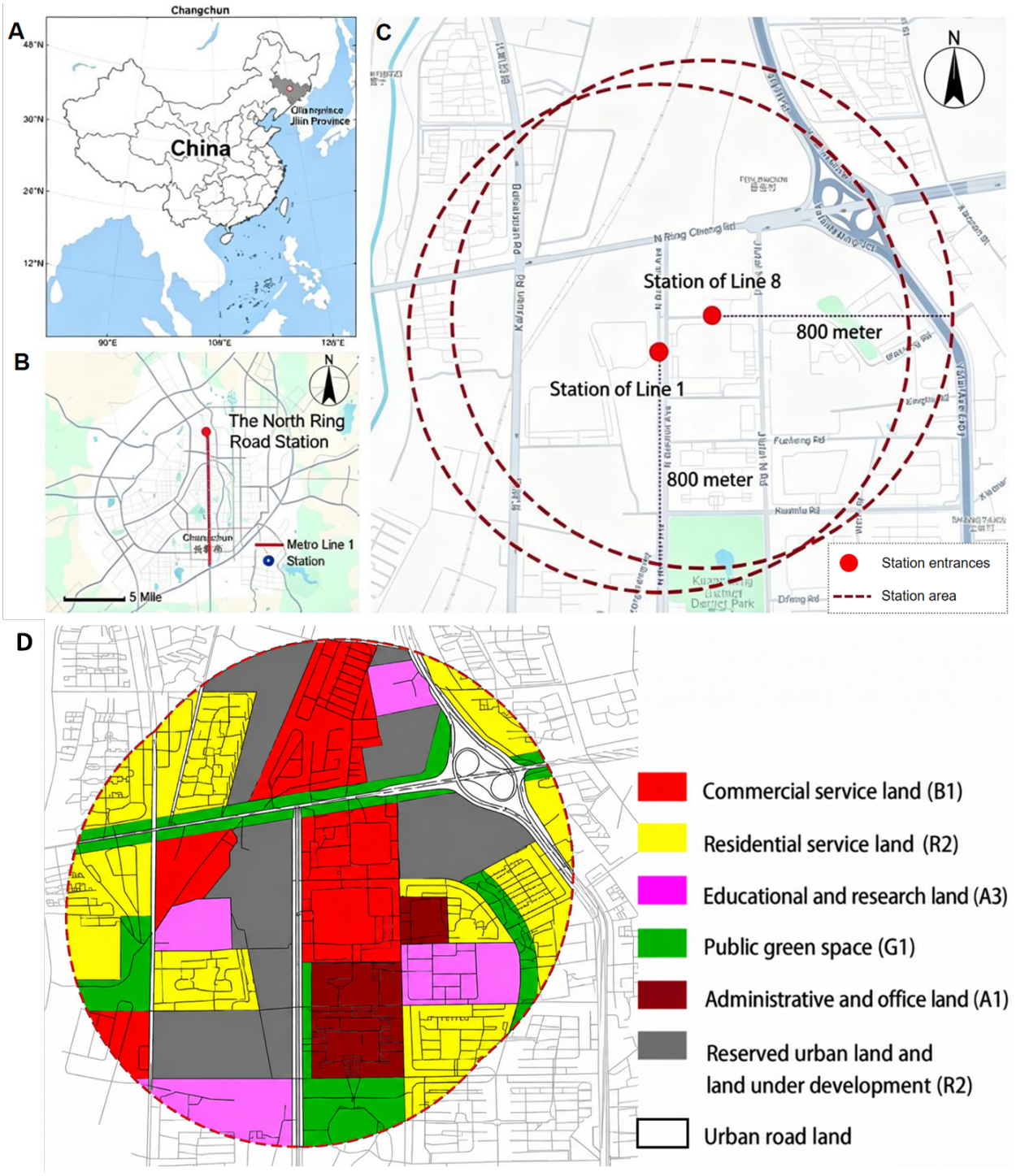


Figure 2. Location and land use structure of the study area around the North Ring Road Station. (A–C) Location of the study area and the 800 m station area boundary. (D) Land use structure within the station area. Source: Map by the authors

per day and 16 heat maps in total. The zoom level was fixed at 18, and the study extent, map orientation, and display scale were kept constant. The images were georeferenced in ArcGIS Desktop using road intersections, building corners, and metro entrances, and projected to WGS 1984/UTM Zone 51N. Raster extent, cell size, and origin were kept consistent. Heat values were assigned using the color-based scheme of Zhang (2021). Blue and light blue were assigned 0, indicating no identifiable heat signal under this scheme, while cyan, green, yellow, orange, and red were converted to progressively higher values according to Zhang (2021). These values represent relative activity intensity rather than actual population density and cannot distinguish commercial consumers from commuters, residents, students, or other users. The eight observations were averaged for each day and extracted to 30 m × 30 m analytical grids. The 30 m grid is an integration unit rather than the native spatial resolution of Baidu Heat Map data. The resulting indicator describes the relative spatial pattern of observed human activity within the station area (Bao *et al.*, 2023). Approximately 57 percent of the analytical grid observations have a converted heat value of zero, indicating no identifiable heat signal under the adopted color-to-value scheme. This high proportion of zero values may affect the distribution of the derived activity indicators and is therefore explicitly considered in the subsequent rank-based analysis and sensitivity tests.

3.3. Grid integration and entrance-based spatial zoning

To integrate commercial function and human activity data within a common analytical framework, the 800 m station area was divided into 30 m × 30 m grids and clipped to the study boundary, yielding 2,704 analytical units (Figure 3A). KDE values for each commercial function and heat-map values from the two sampled days were extracted to the corresponding grids. Spatial zones were defined around the two operational station entrances using Euclidean buffers of 300 m and 500 m, resulting in three zones: the 0–300 m core zone, the 300–500 m transitional zone, and the 500–800 m peripheral zone (Figure 3B). These zones serve as entrance-based analytical distance bands for comparing internal spatial differences and are not intended to represent empirically derived pedestrian catchments. Each grid was assigned to a zone according to its centroid location, resulting in 446, 653, and 1,605 grids, respectively (C. Duan & Chen, 2026; Guo *et al.*, 2024).

3.4. Relative positional change in human activity intensity between sampled weekday and weekend conditions

To account for differences in overall heat levels between the two sampled days and identify changes in each grid's relative position within the station-area activity pattern, *Z*-score standardization was applied separately to the

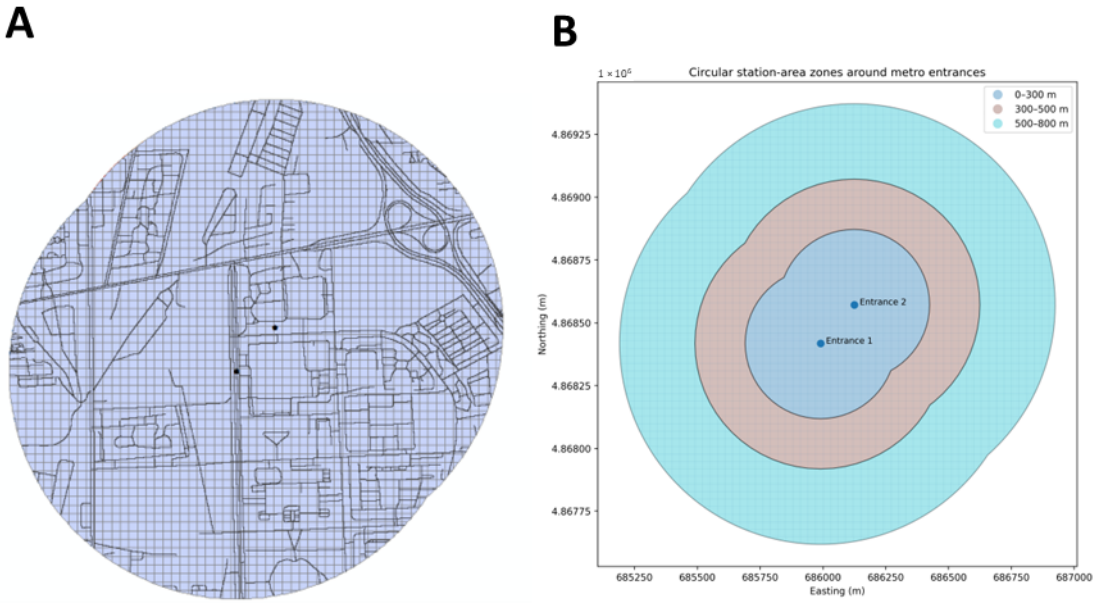


Figure 3. Grid division and spatial zoning of the station area. (A) Grid units within the station area. (B) Spatial zoning of the station area. Source: Map by the authors

mean heat values of the 2,704 grids for each sampling day. *Z*-score standardization was preferred to 0–1 min–max normalization because it preserves the relative position of each grid within the daily activity distribution. The calculation is as follows (**Equations 1 and 2**):

$$Z_{WD,i} = \frac{H_{WD,i} - \bar{H}_{WD}}{SD\left(H_{WD}\right)} \quad (1)$$

$$Z_{WE,i} = \frac{H_{WE,i} - \bar{H}_{WE}}{SD\left(H_{WE}\right)} \quad (2)$$

where the $H_{WD,i}$ and $H_{WE,i}$ terms denote the mean heat values of grid *i*, while the corresponding means and standard deviations are calculated across all grids for each sampling day. The *Z*-score indicates the position of each grid relative to the overall daily activity distribution, thereby reducing the influence of differences in overall heat levels and dispersion between the two days. A relative positional change indicator is then constructed from the difference between the two standardized values as in **Equation 3**.

$$\Delta Z_i = Z_{WE,i} - Z_{WD,i} \quad (3)$$

where, $\Delta Z_i > 0$ indicates that grid *i* occupies a higher relative position on the sampled weekend day, whereas $\Delta Z_i < 0$ indicates a lower relative position. The absolute value of ΔZ_i represents the magnitude of this relative change. Because the two sampling days are standardized separately, the mean *Z*-score for each day is theoretically zero; consequently, the station-wide mean of ΔZ is also theoretically zero, apart from negligible numerical rounding errors. Thus, positive and negative ΔZ values describe a redistribution of relative positions within the study area and do not represent absolute gains or losses in human activity. Because ΔZ is derived from the converted heat-map values, it may be affected by the adopted color-to-value coding and the large number of tied zero values. Therefore, ΔZ is interpreted as a relative positional indicator, and its robustness is assessed using raw heat-value differences and grid-level rank changes.

3.5. Statistical tests

3.5.1. Spatial autocorrelation diagnosis

Global Moran's *I* was used to test spatial autocorrelation in the KDE values of the seven commercial functions, human activity intensity on the two sampled days, and relative positional change (ΔZ) (Moran, 1950). A row-normalized first-order Queen contiguity matrix was used. Statistical significance was tested using 999 random permutations. The test identifies spatial dependence among the grid-based variables and provides the basis for subsequent spatial robustness analysis.

3.5.2. Spearman correlation analysis

Commercial kernel density and heat-map values are both highly skewed, and about 57 percent of the heat-map grids have a value of zero. These zero values indicate no identifiable heat signal under the adopted color-to-value conversion scheme and do not necessarily imply an absence of human activity. The analysis focuses on monotonic relationships between commercial concentration and human activity intensity, so Spearman's rank correlation coefficient was used (Spearman, 1904). At the station-area scale, the seven commercial functions were compared with human activity intensity on the two sampled days. Their associations with relative positional change (ΔZ) were then examined across the core, transitional, and peripheral zones.

3.5.3. Zonal comparison and spatial robustness tests

The Kruskal–Wallis test compared ΔZ distributions across the 0–300 m, 300–500 m, and 500–800 m zones, with ε^2 reported as the effect size. Given spatial dependence, this test was used mainly to describe overall zonal differences rather than as the primary basis for spatial inference.

As Global Moran's *I* indicated significant spatial autocorrelation, spatial block bootstrap was applied to Spearman correlations between commercial KDE and ΔZ within each zone (Lahiri, 2013). Fixed 120 m × 120 m blocks were resampled with replacement for 2,000 iterations to estimate 95 percent confidence intervals for Spearman's ρ. The 120 m block size was retained as the primary setting to preserve sufficient resampling units in the Core Zone. Because the KDE surfaces used a 300 m search radius, larger blocks were also examined in sensitivity tests. The 21 function-by-zone tests were adjusted using the Benjamini–Hochberg false discovery rate (FDR) procedure (Benjamini & Hochberg, 1995).

Core-to-peripheral differences were assessed as $\Delta\rho\text{zone} = \rho_{500–800} - \rho_{0–300}$, with 95 percent confidence intervals estimated by the same bootstrap procedure and the seven comparisons adjusted separately by Benjamini–Hochberg FDR. Sensitivity analyses were conducted to assess the robustness of the results to both spatial block size and the measurement of between-day change. Spatial block sizes of 90, 150, 240, and 300 m were examined against the primary 120 m specification. The function-specific analyses were also repeated using raw heat-value differences and grid-level rank changes to assess dependence on the construction of ΔZ. In addition, grids with no identifiable heat signal on

both sampled days were excluded, and the analyses were repeated. Percentage change was not used because zero baseline values would produce unstable ratios.

3.5.4. Software and reproducible implementation

Spatial data processing and analysis were conducted primarily in ArcGIS Desktop using WGS 1984/UTM Zone 51N (EPSG:32651). The statistical analyses and spatial robustness tests were run in Python (3.12.2, Python Software Foundation, Netherlands) with GeoPandas, pandas, NumPy, SciPy, and statsmodels.

4. Results

4.1. Baseline patterns of commercial functions and human activity

4.1.1. Spatial agglomeration of commercial functions

Shopping is the largest category among the 951 commercial and service POIs, with 419 records (44.06%), followed by food and beverage with 239 (25.13%). Together they make up 69.19 percent of the total (Table 1). The main concentration lies around the metro entrances and the large commercial complex to the south, while a smaller cluster occurs near the northern wholesale market (Figures 4 and 5). Daily life services, food and beverage, and healthcare also appear as smaller nodes in nearby residential areas. Rather than forming a simple single-center pattern, the POIs show a strong core, street-based extensions, a specialized sub-center, and several community-level nodes. Most POIs extend along a northeast–southwest axis, although the pattern varies by function. Shopping shows little directional tendency. Most other functions are oriented northwest–southeast, with food and beverage and daily life services extending farther into peripheral areas. Healthcare occurs in several separate clusters, while accommodation is more compact. The KDE and standard deviational ellipse results do not show a simple decline with distance from the North Ring Road Station. Commercial concentration remains strongest in the core, but individual functions extend outward in different directions.

4.1.2. Spatial patterns of human activity under sampled weekday and weekend conditions

Figure 6 shows differences in the observed intraday activity profiles of the two sampled days. On the sampled weekday, activity was concentrated near the metro station and commercial areas during 08:00–10:00 and 16:00–18:00. After 20:00, activity spread toward nearby residential areas. On the sampled weekend day, activity remained relatively strong from 12:00 to 20:00, while surrounding residential areas and communities also showed higher activity intensity in the afternoon and evening. Similar forms of temporal variation have been reported in previous studies (Miao & Zhou, 2025; Tang & Ta, 2022), although the present observations describe only the two sampled days examined here.

Despite these differences, the overall spatial structure was broadly similar across the two sampled days (Figure 7). High activity was concentrated around metro entrances, major commercial facilities, and activity corridors, with local activity nodes near residential entrances, community commercial areas, and public spaces in the periphery, reflecting a stable core with local spatial heterogeneity (Yanxiao Jiang *et al.*, 2024; Xu *et al.*, 2025). Mean heat values were higher on the sampled weekend day in all three zones, from 79.51 to 89.13 in the Core Zone, 21.98 to 23.69 in the Transitional Zone, and 15.25 to 21.86 in the Peripheral Zone. The main activity center remained in the core, while the magnitude of the between-day difference was larger in the periphery. Because these unstandardized heat values describe activity intensity, ΔZ is used below to examine changes in relative spatial position.

4.1.3. Spatial autocorrelation of major variables

Global Moran's I indicated significant positive spatial autocorrelation for all major variables. Moran's I ranged from 0.977 to 0.983 for the seven commercial KDE surfaces, while mean heat values for the sampled weekday and sampled weekend day were 0.921 and 0.920, respectively; ΔZ had a value of 0.793 (permutation p = 0.001 for all tests). Thus, the 2,704 grids cannot be treated as independent observations. Spatial block bootstrap was therefore used for robust inference on zonal associations between commercial functions and ΔZ.

Table 1. Composition of commercial and service points of interest (POIs)

Commercial function	Number of POIs	Proportion
Shopping	419	44.06%
Food and beverage	239	25.13%
Daily life services	133	13.99%
Sports and recreation	50	5.26%
Education and culture	49	5.15%
Healthcare	37	3.89%
Accommodation	24	2.52%

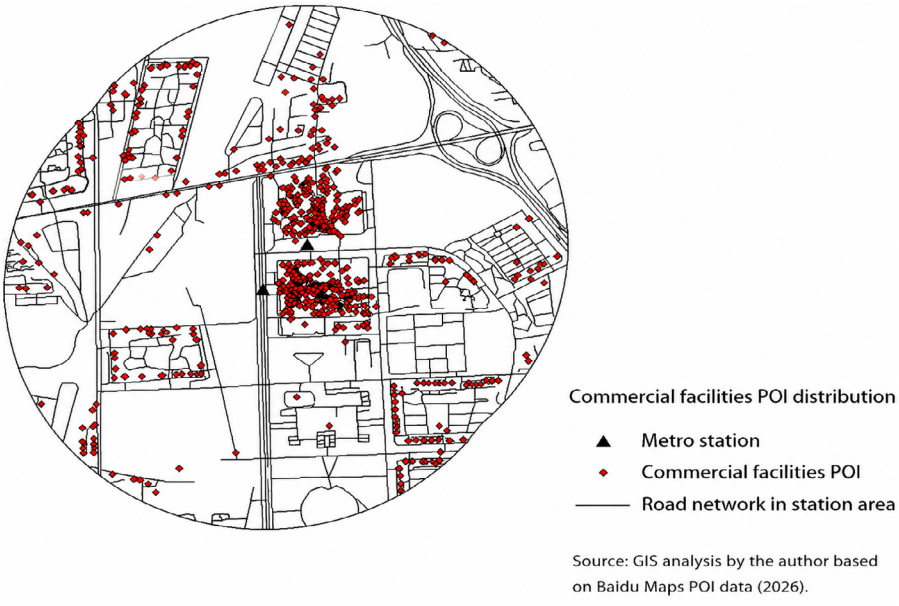


Figure 4. Distribution of commercial points of interest (POIs) within the 800 m analytical station area. Source: Map by the authors

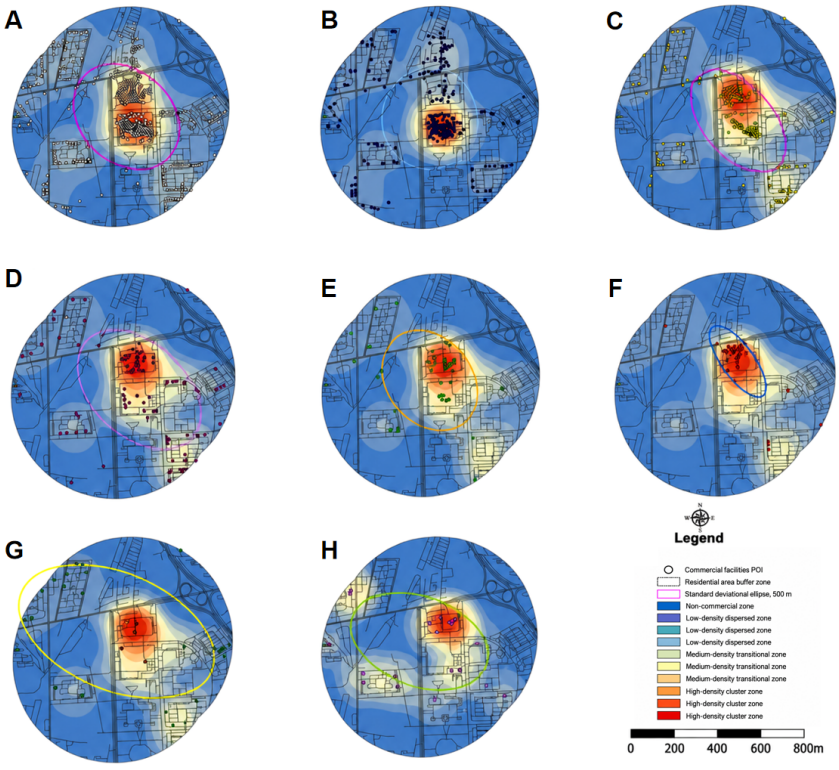


Figure 5. Kernel density estimation and standard deviational ellipse analyses of commercial facilities in the station area. (A) Overall commercial facilities. (B) Shopping. (C) Food and beverage. (D) Daily life services. (E) Sports and recreation. (F) Education and culture. (G) Healthcare. (H) Accommodation. Source: Map by the authors

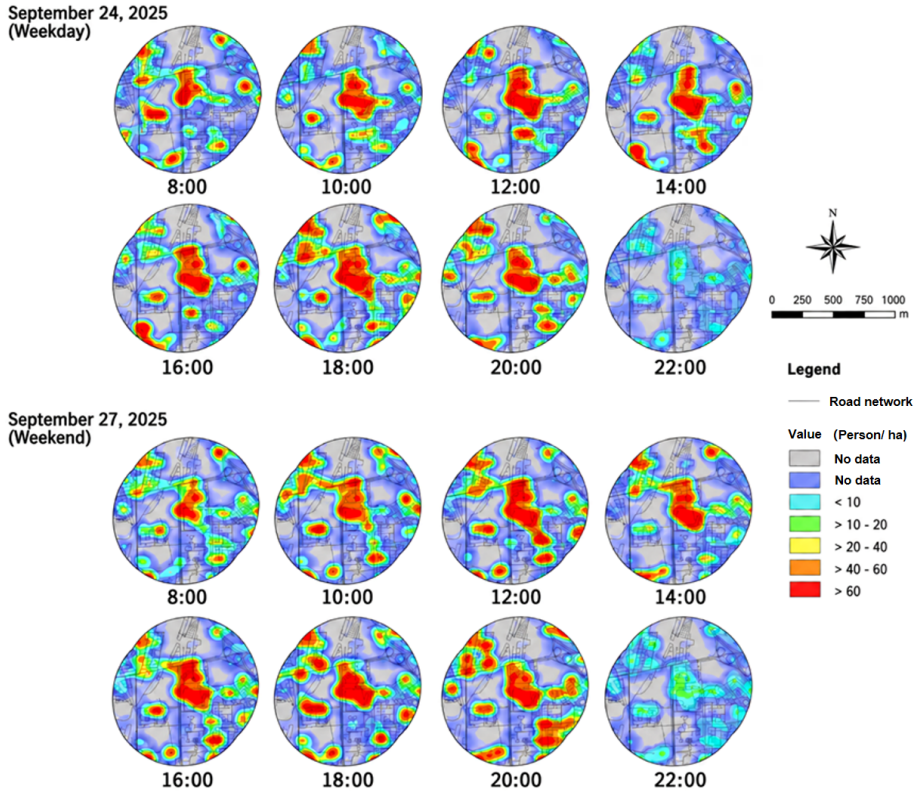


Figure 6. Temporal patterns of human activity under sampled weekday and weekend conditions. Source: Map by the authors

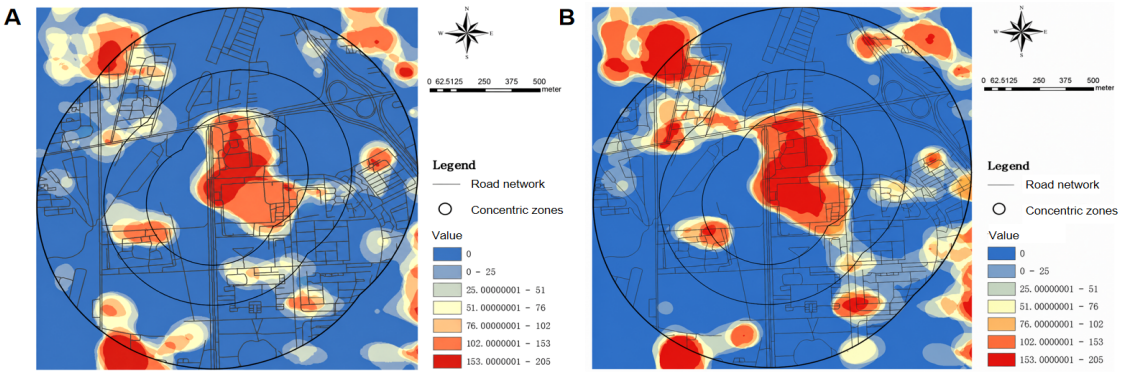


Figure 7. Mean human activity intensity and spatial zones under sampled weekday and weekend conditions. (A) Weekday. (B) Weekend. Source: Map by the authors

4.2. Commercial functions and human activity across the two sampled days

As shown in Table 2 and Figure 8, all seven commercial functions were positively associated with human activity intensity on both sampled days. On the sampled weekday, food and beverage (ρ = 0.573) and daily life services (ρ = 0.547) showed the strongest correlations; on the sampled weekend day, daily life services (ρ = 0.640) and food and beverage (ρ = 0.620) ranked highest. Although shopping accounted for 44.06 percent of all POIs, its correlation was not the strongest, indicating that facility quantity alone does not represent the spatial correspondence between

commercial functions and actual space use. Overall, the correlations were similar in direction and ranking across the two days, with limited differences in magnitude. This broadly stable station-wide relationship provides a reference for identifying local variation that may be less visible in aggregate comparisons. The following analysis therefore uses ΔZ to examine relative positional and function-specific differences across spatial zones.

4.3. Zonal differentiation in relative activity position

As shown in Table 3, ΔZ shifts from negative values in the core and transitional zones to a positive value in the periphery. Mean ΔZ is −0.085 in the 0–300 m Core Zone, −0.059 in the 300–500 m Transitional Zone, and +0.048 in the 500–800 m Peripheral Zone. Although the core retains the highest human activity intensity on both sampled days, its relative position is lower in the September 27

Table 2. Station-area Spearman correlations between commercial kernel density estimation variables and human activity intensity under sampled weekday and weekend conditions (n = 2,704)

Commercial function	Sampled weekday (ρ)	Sampled weekend (ρ)
Shopping	0.420	0.455
Food and beverage	0.573	0.620
Daily life services	0.547	0.640
Sports and recreation	0.453	0.511
Education and culture	0.391	0.401
Healthcare	0.471	0.541
Accommodation	0.386	0.469

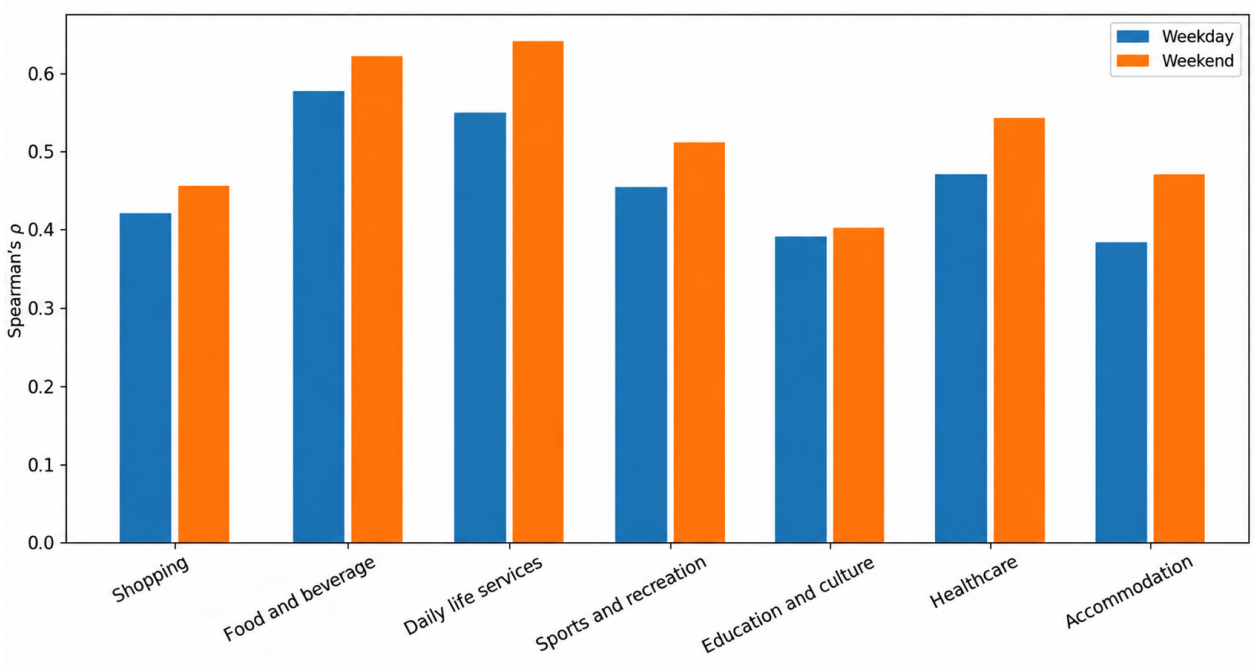


Figure 8. Station-area Spearman correlations between commercial kernel density estimation variables and human activity (n = 2,704) intensity under sampled weekday and weekend conditions. Source: Diagram by the authors

observation than in the September 24 observation, while some peripheral areas occupy relatively higher positions. The Kruskal–Wallis test indicates differences in ΔZ among the three zones ($H = 42.656$, $p < 0.001$), but this result is treated mainly as descriptive given the spatial dependence of the grid data. The small effect size ($\varepsilon^2 = 0.015$) suggests that overall zonal differences are limited. Relative positional change therefore cannot be explained by a simple core-to-periphery gradient (Kruskal & Wallis, 1952).

Figure 9 shows that ΔZ does not follow a regular concentric gradient but displays clear local variation. Low or negative values are concentrated around the metro entrances and commercial core, while positive values occur more often in the northwestern, northern, and southeastern periphery. These positive areas partly overlap with residential land, the northern specialized market, and community-oriented nodes of daily life services, food and beverage, and healthcare. Thus, the core-to-periphery contrast reflects only a broad tendency. Within-zone variation also suggests that distance alone does not account for the observed pattern.

Table 3. Human activity intensity and relative positional change between sampled weekday and weekend conditions across the three spatial zones

Spatial zone	*n*	Sampled weekday mean heat	Sampled weekend mean heat	Mean (ΔZ)
0 to 300 m	446	79.51	89.13	−0.085
300 to 500 m	653	21.98	23.69	−0.059
500 to 800 m	1,605	15.25	21.86	+0.048

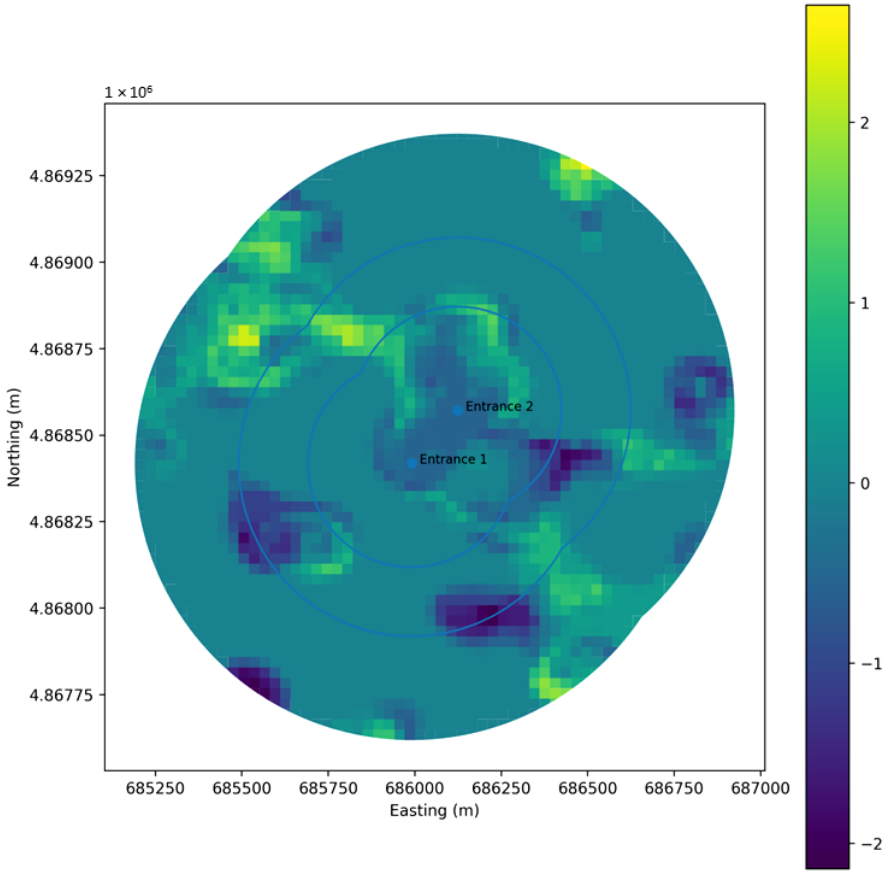


Figure 9. Spatial distribution of relative positional change in human activity intensity between sampled weekday and weekend conditions. Source: Diagram by the authors

4.3.1. Core Zone: High baseline activity intensity and a weaker relative advantage

Within the 0–300 m Core Zone, commercial functions generally show negative or weak associations with ΔZ (Table 4). Shopping and healthcare exhibit spatially robust negative associations, while food and beverage shows only a marginal negative tendency; the remaining functions are weakly related to ΔZ. Thus, locations with stronger commercial concentration tend to occupy lower relative positions on the sampled weekend day.

This does not indicate a decline in raw human activity intensity in the Core Zone. The core retains the highest activity intensity on both sampled days; the negative associations instead indicate a narrowing of its relative advantage as other locations gain prominence. Previous studies have also identified spatial heterogeneity in relationships between station-area functions, built environment characteristics, and vitality (Xu *et al.*, 2025), and the role of commercial configuration around rail transit nodes (Sun *et al.*, 2025). Overall, the core combines high baseline activity intensity with a weaker relative advantage, reflecting adjustment within the station-area pattern.

4.3.2. Transitional Zone: Mixed associations with relative positional change

Within the 300–500 m Transitional Zone, associations between commercial functions and ΔZ were mixed (Table 5). Education and culture show a significant negative correlation with ΔZ, while accommodation and sports and recreation show positive tendencies. Shopping, food and beverage, daily life services, and healthcare have weaker correlations, indicating no consistent functional pattern. A weak association with ΔZ does not imply a weak relationship with human activity intensity. For example, food and beverage remains strongly correlated with activity intensity on both sampled days but is almost unrelated to ΔZ. Overall, the Transitional Zone is characterized more by function-specific variation than by a common directional change.

4.3.3. Peripheral Zone: Multifunctional co-occurrence and greater relative prominence on the sampled weekend day

Within the 500–800 m Peripheral Zone, most commercial functions show positive correlations with ΔZ (Table 6). Food and beverage, daily life services, sports and recreation, education and culture, healthcare, and accommodation exhibit significant positive associations, while shopping shows a weaker positive correlation. Although the coefficients are modest, their consistent direction indicates that several service and leisure functions are associated with higher relative positions on the sampled weekend day. Correlation strength does not match POI counts. Accommodation has the fewest POIs but the highest correlation with ΔZ ($\rho = 0.275$), whereas shopping has the most POIs but a weaker correlation ($\rho = 0.160$). This further indicates that facility quantity alone cannot explain variation in relative activity position.

Figure 10 shows that functional associations vary noticeably across the three zones, but these changes do not follow a simple distance-based gradient. The shifts are particularly evident for shopping, food and beverage, daily life services, sports and recreation, and healthcare. These shifts are examined further through core and peripheral comparisons.

4.4. Changes in functional associations across zones and synthesis of results

4.4.1. Core to peripheral shifts in functional associations

Core and peripheral correlations were compared to assess cross-zonal changes in the relationships between commercial functions and ΔZ (Table 7; Figure 11). Shopping, food and beverage, daily life services, sports and recreation, and healthcare showed significant positive $\Delta\rho$ values, with 95 percent confidence intervals excluding zero and FDR-adjusted $q < 0.05$. Healthcare showed the largest shift ($\Delta\rho = +0.522$), followed by shopping and food and beverage. Education and culture and accommodation also shifted positively, but with weaker statistical evidence. A larger $\Delta\rho$ indicates a change in association rather than a strong peripheral correlation itself. For example, shopping shifted from $\rho = -0.312$ in the core to $\rho = +0.160$ in the periphery. These shifts reveal function-specific spatial differences that are less visible in the broadly stable station-wide correlations.

Sensitivity analyses supported the stability of the main core-to-peripheral association patterns across alternative specifications. Analyses using 240 m and 300 m spatial blocks retained generally consistent association directions, although the larger blocks reduced the number of effective resampling units in the Core Zone. Analyses based on raw heat-value differences and grid-level rank changes reproduced the principal spatial tendencies identified using ΔZ. Excluding grids with no identifiable heat signal on both sampled days did not materially alter the main core-to-peripheral association patterns. These results indicate that the main findings are not highly sensitive to the specific construction of ΔZ or to persistent zero-valued grids, although uncertainty associated with heat-map conversion remains.

Table 4. Correlations between commercial kernel density estimation and relative positional change in the Core Zone (0–300 m) with spatial block bootstrap results

Commercial function	Spearman's ρ	120 m spatial block 95% confidence interval	Benjamini–Hochberg-adjusted *q*
Shopping	−0.312	[−0.491, −0.087]	0.033
Food and beverage	−0.220	[−0.404, +0.002]	0.091
Daily life services	−0.112	[−0.335, +0.139]	0.531
Sports and recreation	−0.106	[−0.343, +0.137]	0.584
Education and culture	−0.016	[−0.279, +0.240]	0.991
Healthcare	−0.293	[−0.484, −0.087]	0.021
Accommodation	+0.007	[−0.228, +0.240]	0.997

Table 5. Correlations between commercial kernel density estimation and relative positional change in the Transitional Zone (300–500 m) with spatial block bootstrap results

Commercial function	Spearman's ρ	120 m spatial block 95% confidence interval	Benjamini–Hochberg-adjusted *q*
Shopping	+0.046	[−0.147, +0.258]	0.784
Food and beverage	+0.006	[−0.213, +0.247]	0.991
Daily life services	+0.045	[−0.178, +0.249]	0.793
Sports and recreation	+0.151	[−0.030, +0.342]	0.153
Education and culture	−0.283	[−0.453, −0.062]	0.021
Healthcare	−0.056	[−0.275, +0.147]	0.784
Accommodation	+0.197	[+0.004, +0.373]	0.080

Table 6. Correlations between commercial kernel density estimation and relative positional change in the Peripheral Zone (500–800 m) with spatial block bootstrap results

Commercial function	Spearman's ρ	120 m spatial block 95% confidence interval	Benjamini–Hochberg-adjusted *q*
Shopping	+0.160	[+0.022, +0.300]	0.061
Food and beverage	+0.246	[+0.106, +0.372]	0.011
Daily life services	+0.268	[+0.126, +0.395]	<0.001
Sports and recreation	+0.269	[+0.122, +0.410]	<0.001
Education and culture	+0.229	[+0.067, +0.367]	0.021
Healthcare	+0.229	[+0.073, +0.377]	0.021
Accommodation	+0.275	[+0.119, +0.412]	<0.001

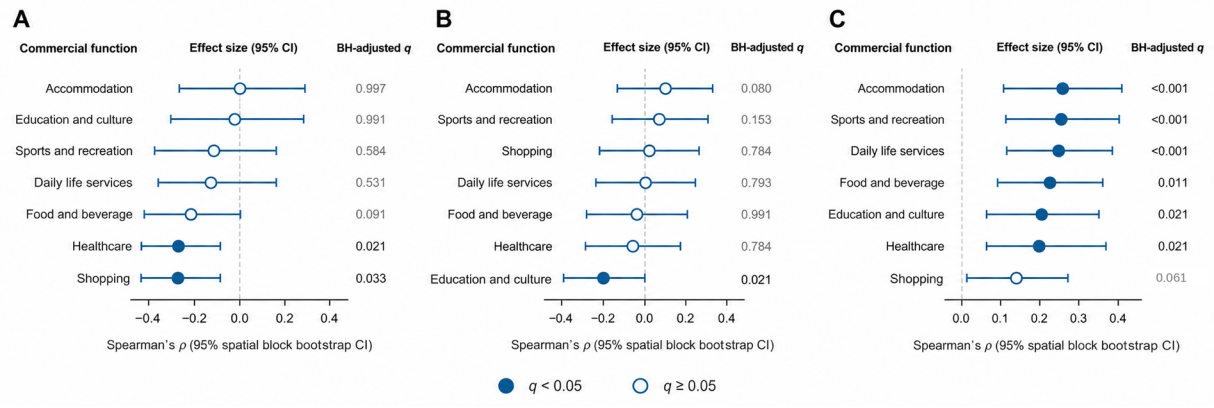


Figure 10. Spearman correlation coefficients between commercial kernel density estimation and relative positional change across the three zones, with 95 percent CIs from a 120 m spatial block bootstrap. (A) Core Zone. (B) Transitional Zone. (C) Peripheral Zone
Abbreviations: BH: Benjamini–Hochberg; CI: Confidence intervals. Source: Diagram by the authors

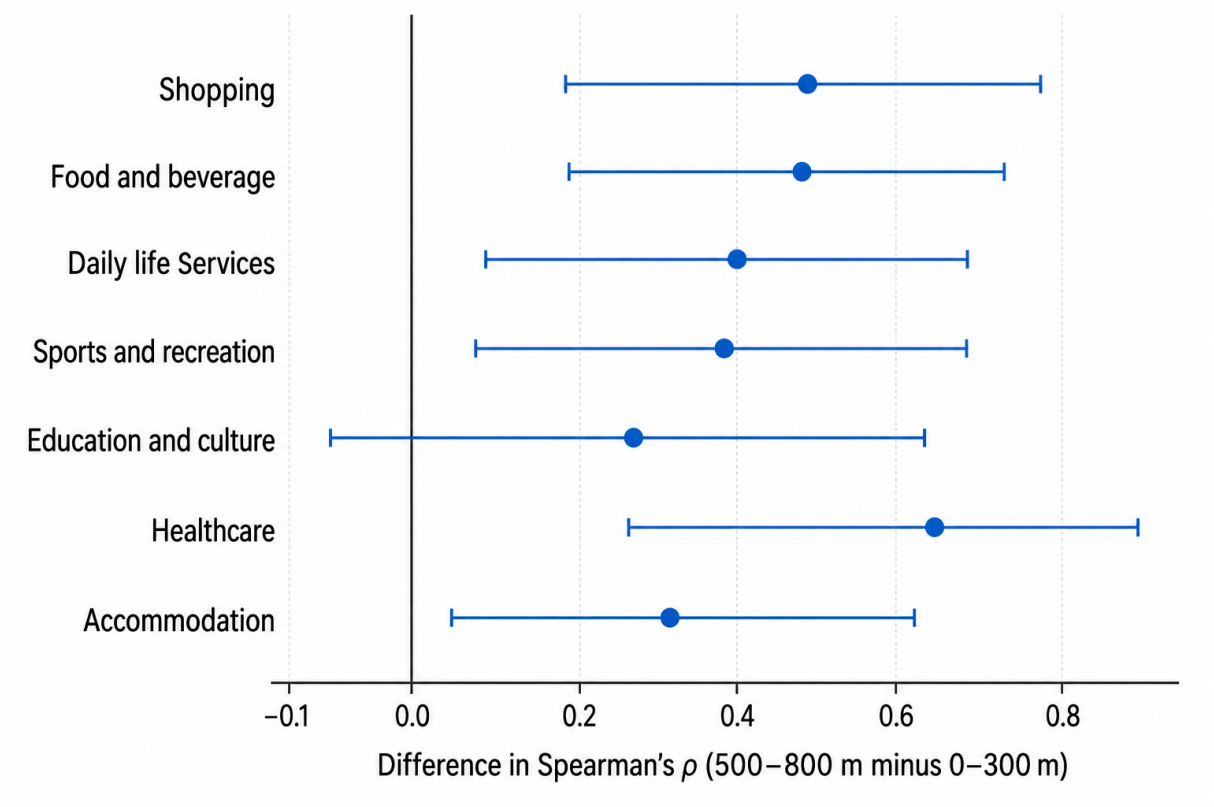


Figure 11. Core-to-peripheral differences in associations between commercial functions and relative positional change, with 95 percent confidence intervals from a 120 m spatial block bootstrap. Source: Diagram by the authors

Table 7. Spatial block bootstrap comparison of commercial kernel density estimation–relative positional change correlations between the Core and Peripheral Zones

Commercial function	Core Zone (ρ)	Peripheral Zone (ρ)	$\Delta\rho_{zone}$ (Peripheral–Core)	95% confidence interval	FDR-adjusted *q*
Shopping	−0.312	+0.160	+0.473	[+0.208, +0.691]	<0.001
Food and beverage	−0.220	+0.246	+0.467	[+0.213, +0.702]	0.002
Daily life services	−0.112	+0.268	+0.380	[+0.104, +0.643]	0.007
Sports and recreation	−0.106	+0.269	+0.376	[+0.087, +0.645]	0.011
Education and culture	−0.016	+0.229	+0.245	[−0.068, +0.553]	0.117
Healthcare	−0.293	+0.229	+0.522	[+0.269, +0.759]	<0.001
Accommodation	+0.007	+0.275	+0.269	[−0.039, +0.542]	0.083

Abbreviation: FDR: False discovery rate

4.4.2. Temporal and zonal association patterns of commercial functions

Considering association direction, spatial robustness, and core-to-peripheral shifts, the seven commercial functions can be descriptively grouped into three patterns. Shopping and healthcare shift from negative associations with ΔZ in the core to positive associations in the periphery. Food and beverage, daily life services, and sports and recreation show stronger positive associations in the Peripheral Zone. Education and culture and accommodation show less consistent patterns, with weaker statistical evidence for clear core-to-peripheral differences. Thus, similar station-wide relationships can mask different association patterns across internal spatial zones.

These results indicate that relationships between commercial functions and relative activity position vary across spatial contexts. For the same function, both the direction and strength of association can differ by zone, consistent with previous evidence of scale dependence and spatial heterogeneity in metro station areas (Guo *et al.*, 2024; J. Wang *et al.*, 2025).

5. Discussion

5.1. Overall stability and local restructuring of relative patterns

At the station-area scale, all seven commercial functions were positively correlated with human activity intensity on both sampled days, and the correlation structures were largely similar. This indicates that areas with high commercial concentration remained important activity spaces under both sampled conditions, consistent with previous findings on spatial links between commercial facilities, functional agglomeration, and urban activities (Shi *et al.*, 2020; Tang & Ta, 2022). The differences observed between the two sampled days therefore occurred within a broadly stable spatial structure rather than through a major shift in the main activity center.

Within this stable structure, ΔZ reveals changes in relative positions of individual spatial units. Overall zonal differences are small, but specific commercial functions vary more clearly across the core, transitional, and peripheral zones. Overall stability and local restructuring can therefore coexist. Pedestrian networks, spatial interfaces, and local accessibility may help explain these differences (Guo et al., 2024; Sevtsuk, 2014), although they are not directly tested. Human activity intensity and relative positional change capture different aspects of the spatial pattern and reveal localized differences less visible in station-wide comparisons.

5.2. Zonal context and functional differentiation

The zonal effect is small ($\varepsilon^2 = 0.015$), and distance explains only a small share of the relative positional differences observed between the two sampled days. Commercial concentration, residential demand, road conditions, and destination type vary across the three zones. Guo *et al.* (2024) found similar scale-related differences between the built environment and station-area vitality. Accordingly, function-specific associations with relative activity position may vary across spatial settings (Pan & Huang, 2024).

Negative associations with ΔZ occur for shopping and healthcare in the core. Activity intensity is already high around metro entrances, major commercial facilities, and key destinations, which may help explain weaker relative positions on the sampled weekend day. Large blocks, wide roads, and enclosed interfaces may provide spatial context, although their effects were not directly tested. In the periphery, residential communities and everyday activity spaces are common, while food and beverage,

daily life services, and sports and recreation show stronger positive associations with ΔZ. These patterns may reflect differences in local demand and spatial context.

The differences observed between the two sampled days are not fully described by distance alone. Functional type and local spatial context may also help interpret the observed variation. The small overall zonal effect and clearer functional differences further suggest that function type should be interpreted together with its surrounding spatial context.

5.3. Interpretation and potential planning relevance

The results identify spatial associations between commercial functions and relative positional change across different zones (Table 8). In the 0–300 m Core Zone, shopping and healthcare showed negative associations with ΔZ despite high baseline activity intensity. This pattern suggests that future research could examine whether local spatial conditions, such as pedestrian connectivity, street–building interfaces, crossing conditions, and the organization of major destinations, are related to these associations. These factors were not directly measured in this study and therefore require further empirical evaluation.

In the 500–800 m Peripheral Zone, food and beverage, daily life services, and sports and recreation showed more positive associations with relative positional change. This pattern suggests that future research could examine whether their relationships with residential areas, community spaces, pedestrian networks, and local service demand are related to the observed peripheral variation. These potential mechanisms require further empirical testing using additional built-environment and behavioral data.

Context-dependent functions, including education and culture and accommodation, may warrant more location-specific consideration of destination characteristics, surrounding land use, and temporal patterns of use.

5.4. Limitations and future research

This study has several limitations. First, temporal replication is limited to one sampled weekday and one sampled weekend day. The eight observations within each day characterize intraday variation but do not constitute independent day-level replication. The observed differences therefore describe an exploratory comparison of the two sampled conditions and should not be generalized to broader weekday–weekend patterns. Repeated observations across multiple weekdays and weekend days, seasons, weather conditions, and event contexts are needed to evaluate temporal generalizability. Second, Baidu heat maps represent platform-detected relative activity and may be affected by user and sampling biases. The color-to-value conversion also introduces measurement uncertainty, with approximately 57 percent of grid observations coded as zero, indicating no identifiable heat signal rather than confirmed absence of activity. Sensitivity analyses using raw heat-value differences, grid-level rank changes, and exclusion of grids with no identifiable signal on both sampled days were therefore conducted, although some uncertainty remains. The data do not provide information on user characteristics or activity purposes, and the 30 m grid is an analytical integration unit rather than the native resolution of the heat-map data. Third, commercial concentration was estimated with a fixed 300 m KDE bandwidth, and the seven POI categories are unevenly represented. These choices may affect the strength of function-specific associations. The 300, 500, and 800 m zones are also Euclidean, entrance-based bands rather than network-based pedestrian catchments, so the thresholds may not transfer directly to other stations. Future work should combine repeated heat-map observations with pedestrian counts or visitor surveys, test alternative bandwidths and network catchments, and compare multiple stations with different urban contexts. Such extensions would help assess both temporal robustness and spatial transferability.

Table 8. Sampled-day activity characteristics and potential planning relevance across spatial zones

Spatial zone	Main findings	Spatial diagnosis	Potential planning relevance
0 to 300 m Core Zone	Highest human activity intensity; mean $\Delta Z = -0.085$; shopping and healthcare negatively associated with ΔZ	High baseline activity intensity, weaker relative advantage	Consider pedestrian links and interface continuity between metro entrances, commercial destinations, and streets, alongside facility provision
300 to 500 m Transitional Zone	Mean $\Delta Z = -0.059$; most functions weakly related to ΔZ	Weak association between baseline activity intensity and relative positional change	Consider pedestrian and functional connections, together with daily services and staying spaces where locally appropriate
500 to 800 m Peripheral Zone	Mean $\Delta Z = +0.048$; multiple daily functions positively related to ΔZ	Lower activity intensity, greater relative prominence on the sampled weekend day	Consider distributed community-oriented service nodes for food, daily services, and recreation, with attention to links with housing, public space, and walking networks

6. Conclusion

The main conclusions are as follows: first, although relative positions within the station area changed, the overall relationship between commercial functions and human activity intensity remained broadly stable across the two sampled days. Areas around the metro entrances and the commercial core retained the highest activity intensity. Mean ΔZ was −0.085 in the Core Zone (0–300 m) and +0.048 in the Peripheral Zone (500–800 m). The core therefore showed a weaker relative advantage, while some peripheral areas gained relative prominence within the station-area activity distribution. These changes occurred within a broadly stable spatial structure rather than indicating a clear shift of the main activity center.

Second, relative positional change did not follow a simple distance gradient. Although ΔZ differed across the three zones, the overall zonal effect was small (ε^2 = 0.015). Clearer differences emerged at the functional level. Shopping, food and beverage, daily life services, sports and recreation, and healthcare showed distinct core-to-peripheral shifts in their associations with ΔZ. The observed variation is not fully described by distance alone, and local spatial context may also help interpret these differences.

Third, the observed associations provide a basis for further planning and urban-design evaluation. The contrasting core and peripheral patterns suggest that future studies should examine the roles of pedestrian connectivity, built-environment conditions, residential context, and local service demand. Because these factors were not directly measured and the analysis is based on a single station and two sampled days, the findings should be interpreted as exploratory rather than as causal or general planning recommendations. Further repeated observations and multi-station validation are therefore needed.

Acknowledgments

None.

Funding

This study was supported by Universiti Malaysia Sabah under the UMSGreat Grant (GUG0665-1/2024), entitled "Enhancing the Commercial Vitality of Changchun Rail Transit Through Transit-Oriented Development." Additional support was provided by the Scientific Research Project of the Jilin Provincial Department of Education (Grant No. JJKH20262033SZ), entitled "A Three-Stage Integrated Education Mechanism for the 'Great Ideological and Political Course' in Higher Education"; the Graduate Education and Teaching Reform Research Project of Beihua University (Grant No. JG[2025]035), entitled "Digital-Intelligent Integration Mechanism for the Graduate 'Great Ideological and Political Course'"; and the 2025 Jilin Provincial College Student Innovation and Entrepreneurship Training Program (Grant No. S202510201117), entitled "Empowering Spatial Vitality through Multi-Source Data: Influencing Factors and Optimization Strategies for the Section from Songhua River Catholic Church to Yuwen Middle School in Jilin City."

Conflict of interest

The authors declare no conflicts of interest.

Author contributions

Conceptualization: Danwei Zhao, Ahmad Nurfaidhi Rizalman
Data curation: Danwei Zhao, Linxi Zeng, Qiuyu Zhao, Pengbo Li
Formal analysis: Danwei Zhao
Investigation: Danwei Zhao, Linxi Zeng, Qiuyu Zhao, Pengbo Li
Methodology: Danwei Zhao, Ahmad Nurfaidhi Rizalman
Project administration: Danwei Zhao
Supervision: Ahmad Nurfaidhi Rizalman
Visualization: Danwei Zhao, Linxi Zeng, Qiuyu Zhao, Pengbo Li
Writing–original draft: Danwei Zhao
Writing–review & editing: Danwei Zhao, Ahmad Nurfaidhi Rizalman

Ethics approval and consent to participate

Not applicable.

Consent for publication

Not applicable.

Availability of data

The data that support the findings of this study are available from publicly accessible sources and from the corresponding author upon reasonable request.

Further disclosure

AI-assisted technologies were used only for language polishing and readability improvement. The authors reviewed and edited the manuscript and take full responsibility for the final content.

References

Abudurexiti, A., Abulikemu, Z., & Keyimu, M. (2025). POI-based assessment of sustainable commercial development:

Spatial distribution characteristics and influencing factors of commercial facilities around Urumqi Metro Line 1 stations. *Sustainability*, *17*(12), 5270.

https://doi.org/10.3390/su17125270

Bao, W., Gong, A., Zhang, T., Zhao, Y., Li, B., & Chen, S. (2023). Mapping population distribution with high spatiotemporal resolution in Beijing using Baidu Heat Map data. *Remote Sensing*, *15*(2), 458.

https://doi.org/10.3390/rs15020458

Benjamini, Y., & Hochberg, Y. (1995). Controlling the false discovery rate: A practical and powerful approach to multiple testing. *Journal of the Royal Statistical Society: Series B*, *57*(1), 289–300.

https://doi.org/10.1111/j.2517-6161.1995.tb02031.x

Bertolini, L. (1999). Spatial development patterns and public transport: The application of an analytical model in the Netherlands. *Planning Practice & Research*, *14*(2), 199–210.

https://doi.org/10.1080/02697459915724

Bivina, G. R., Gupta, A., & Parida, M. (2020). Walk accessibility to metro stations: An analysis based on meso- or micro-scale built environment factors. *Sustainable Cities and Society*, 55, 102047.

https://doi.org/10.1016/j.scs.2020.102047

Cai, Z. (2026). Urban spatial dynamic modeling in transition: Hybrid, human-centric, and scalable futures. *Ambio*.

https://doi.org/10.1007/s13280-026-02392-0

Cai, Z., Karvonen, A., Cong, C., & Huang, W. (2026). Fine-grained urban land use simulation: Integrating spatial dynamic modeling with a pre-trained vision-language model. *Computers, Environment and Urban Systems*, *126*, 102416.

https://doi.org/10.1016/j.compenvurbsys.2026.102416

Calthorpe, P. (1993). *The next American metropolis: Ecology, community, and the American dream*. Princeton Architectural Press.

Cervero, R., & Kockelman, K. (1997). Travel demand and the 3Ds: Density, diversity, and design. *Transportation Research Part D: Transport and Environment*, *2*(3), 199–219.

https://doi.org/10.1016/S1361-9209(97)00009-6

Duan, C., & Chen, Y. (2026). Delineating public life-oriented metro station catchment areas: A framework integrating empirical observation, street view imagery, and machine learning. *Cities*, *171*, 106865.

https://doi.org/10.1016/j.cities.2026.106865

Duan, J., Wang, H., Liu, L., & Zhang, J. (2025). The attraction gradient of urban functions: How does functional mix at multiple scales predict urban vitality. *Cities*, *156*, 105516.

https://doi.org/10.1016/j.cities.2024.105516

Guo, Z., Luo, K., Yan, Z., Hu, A., Wang, C., Mao, Y., & Niu, S. (2024). Assessment of the street space quality in the metro station areas at different spatial scales and its impact on the urban vitality. *Frontiers of Architectural Research*, *13*(6), 1270–1287.

https://doi.org/10.1016/j.foar.2024.06.006

Hillier, B., Penn, A., Hanson, J., Grajewski, T., & Xu, J. (1993). Natural movement: Or, configuration and attraction in urban pedestrian movement. *Environment and Planning B: Planning and Design*, *20*(1), 29–66.

https://doi.org/10.1068/b200029

Jacobs, J. (1961). *The death and life of great American cities*. Random House.

Jiang, Y., Han, Y., Liu, M., & Ye, Y. (2022). Street vitality and built environment features: A data-informed approach from fourteen Chinese cities. *Sustainable Cities and Society*, *79*, 103724.

https://doi.org/10.1016/j.scs.2022.103724

Jiang, Y., Huang, Z., Zhou, X., & Chen, X. (2024). Evaluating the impact of urban morphology on urban vitality: An exploratory study using big geo-data. *International Journal of Digital Earth*, *17*(1), 2327571.

https://doi.org/10.1080/17538947.2024.2327571

Kruskal, W. H., & Wallis, W. A. (1952). Use of ranks in one-criterion variance analysis. *Journal of the American Statistical Association*, *47*(260), 583–621.

https://doi.org/10.1080/01621459.1952.10483441

Lahiri, S. N. (2013). *Resampling methods for dependent data*. Springer Science & Business Media.

Lahoorpoor, B., & Levinson, D. M. (2020). Catchment if you can: The effect of station entrance and exit locations on accessibility. *Journal of Transport Geography*, *82*, 102556.

https://doi.org/10.1016/j.jtrangeo.2019.102556

Miao, Y., & Zhou, J. (2025). Vibrancy of the space around and between metro stations: Life between Stations and its determinants in Hong Kong. *Transportation*.

https://doi.org/10.1007/s11116-025-10710-w

Montgomery, J. (1998). Making a city: Urbanity, vitality and urban design. *Journal of Urban Design*, *3*(1), 93–116.

https://doi.org/10.1080/13574809808724418

Moran, P. A. P. (1950). Notes on continuous stochastic phenomena. *Biometrika*, *37*(1–2), 17–23.

https://doi.org/10.2307/2332142

Moyano, A., Solís, E., Díaz-Burgos, E., Rodrigo, A., & Coronado, J. M. (2023). Typologies of stations' catchment areas in metropolitan urban peripheries: From car-oriented to sustainable urban strategies. *Land Use Policy*, *134*, 106903.

https://doi.org/10.1016/j.landusepol.2023.106903

Pan, H., & Huang, Y. (2024). TOD typology and station area vibrancy: An interpretable machine learning approach. *Transportation Research Part A: Policy and Practice*, *186*, 104150.

https://doi.org/10.1016/j.tra.2024.104150

Peng, J., Hu, Y., Liang, C., Wan, Q., Dai, Q., & Yang, H. (2023). Understanding nonlinear and synergistic effects of the built environment on urban vibrancy in metro station areas. *Journal of Engineering and Applied Science*, *70*, 18.

https://doi.org/10.1186/s44147-023-00182-z

Sevtsuk, A. (2014). Location and agglomeration: The distribution of retail and food businesses in dense urban environments. *Journal of Planning Education and Research*, *34*(4), 374–393.

https://doi.org/10.1177/0739456X14550401

Shi, P., Xiao, Y., & Zhan, Q. (2020). A study on spatial and temporal aggregation patterns of urban population in Wuhan City based on Baidu Heat Map and POI data. *International Review for Spatial Planning and Sustainable Development*, *8*(3), 101–121.

https://doi.org/10.14246/irspsda.8.3_101

Silverman, B. W. (2018). *Density estimation for statistics and data analysis*. Routledge.

Spearman, C. (1904). The proof and measurement of association between two things. *The American Journal of Psychology*, *15*(1), 72–101.

https://doi.org/10.2307/1422689

Sun, X., Hong, L., & Cools, M. (2025). Modeling pedestrian behavior in metro stations with commercial facilities: An attractiveness-based approach. *Transportation Research Record: Journal of the Transportation Research Board*, *2679*(9), 834–846.

https://doi.org/10.1177/03611981251340389

Tang, S., & Ta, N. (2022). How the built environment affects the spatiotemporal pattern of urban vitality: A comparison among different urban functional areas. *Computational Urban Science*, *2*, 39.

https://doi.org/10.1007/s43762-022-00069-4

Wang, B., Lei, Y., Xue, D., Liu, J., & Wei, C. (2022). Elaborating spatiotemporal associations between the built environment and urban vibrancy: A case of Guangzhou City, China. *Chinese Geographical Science*, *32*(3), 480–492.

https://doi.org/10.1007/s11769-022-1272-6

Wang, J., Liu, Y., & Wei, Z. (2025). The impact of the built environment on the spatial vitality of metro station areas and its heterogeneity: A case study of the four central districts of Guangzhou City. *Progress in Geography*, *44*(8), 1664–1677.

https://doi.org/10.18306/dlkxjz.2025.08.008

Wu, C., Ye, X., Ren, F., & Du, Q. (2018). Check-in behaviour and spatio-temporal vibrancy: An exploratory analysis in Shenzhen, China. *Cities*, *77*, 104–116.

https://doi.org/10.1016/j.cities.2018.01.017

Xia, C., Yeh, A. G. O., & Zhang, A. (2020). Analyzing spatial relationships between urban land use intensity and urban vitality at street block level: A case study of five Chinese megacities. *Landscape and Urban Planning*, *193*, 103669.

https://doi.org/10.1016/j.landurbplan.2019.103669

Xu, Y., Mao, W., & Hu, S. (2025). Unveiling the pulse of urban metro stations: A TOD-driven approach to measuring vibrancy using geographically weighted random forest. *International Journal of Digital Earth*, *18*(1), 2524054.

https://doi.org/10.1080/17538947.2025.2524054

Yan, C., Gao, Y., & Yang, Y. (2024). Exploring the spatial patterns of accessibility to metro services considering the locations of station entrances/exits. *Buildings*, *14*(11), 3532.

https://doi.org/10.3390/buildings14113532

Yue, Y., Zhuang, Y., Yeh, A. G. O., Xie, J.-Y., Ma, C.-L., & Li, Q.-Q. (2017). Measurements of POI-based mixed use and their relationships with neighbourhood vibrancy. *International Journal of Geographical Information Science*, *31*(4), 658–675.

https://doi.org/10.1080/13658816.2016.1220561

Zhang, H. (2021). Extracting active population data based on Baidu Heat Maps for transportation planning applications. *Urban Transport of China, 19*(3), 103–111.

https://doi.org/10.13813/j.cn11-5141/u.2021.0306-en